

## Understanding Backspatter due to Skull Fracture from a Ballistic Projectile

**Raj Das<sup>1,\*</sup>, Justin Fernandez<sup>2</sup>, Alistair Collins<sup>1</sup>, Anurag Verma<sup>1</sup>, Michael Taylor<sup>3</sup>**

<sup>1</sup>Department of Mechanical Engineering, University of Auckland, Auckland 1010, New Zealand

<sup>2</sup>Auckland Bioengineering Institute, University of Auckland, Auckland 1010, New Zealand

<sup>3</sup>Institute of Environmental Science and Research (ESR), Christchurch 8041, New Zealand

\* Corresponding author: r.das@auckland.ac.nz

---

**Abstract** In forensics, a challenge arises from relating observed evidence to the actual events. Specifically, in cranial wounds resulting from a gunshot, the study of backspatter patterns (material propagated opposite to the direction of the projectile) can provide information about the cause by linking material to the firearm, shooter or surrounding objects. Firstly, this study investigates the physics during backspatter from a high speed projectile impact by evaluating two skull simulant materials. Secondly, we evaluate the suitability of a mesh-free method called Smoothed Particle Hydrodynamics (SPH) to model the fracturing and splashing mechanism during backspatter.

The study has shown that projectile impact causes fragmentation of material at the impact site, whilst transferring momentum to fragmented particles. The particles travel along the path of least resistance, leading to partial material movement in the reverse direction of the projectile causing backspatter. The amount of backspatter depends on the strain limit of each material and how rapidly the bullet hole closes. The path of resistance is dependent on the constitutive properties of the materials. MDF was found to be a better simulant for a human skull than polycarbonate as demonstrated by the backspatter pattern. SPH was a suitable numerical method for modeling the high speed impact fracture, fragmentation during backspatter. The simulation predictions agreed well to the experimental data of medium density fiberboard (MDF).

**Keywords** Backspatter, cranial injury, skull simulant, impact, SPH.

---

### 1. Introduction

Wound ballistics is the study of phenomena that arises when a projectile strikes and penetrates a human or animal [1]. Due to variability in biological wounds from projectiles, computational predictions are increasingly playing a role in drawing conclusions. One important feature of wound ballistics is ‘backspatter’, a term used to describe any tissue ejected from a gunshot entrance in the opposite direction to the line of fire [2, 3]. However, while well documented, backspatter mechanics is not fully understood and involves multiple factors including transfer of kinetic energy, rapid expansion of gas, and high deformation of biological material.

Following a firearm discharge, “high velocity” blood spatter [4] is created and often characterised by a finely spattered pattern [2]. The spatter pattern is usually circular when the projectile is at right angles to the surface and a narrow elongated pattern forms when the projectile is at narrower angles [5]. These larger elongated patterns may be analysed to determine the angle of impact and origin [5, 6]. The distance travelled by backspatter is reported as highly variable in the literature. For example, close gunshots to the head of live calves produced backspatter between 0-50 cm with a maximum distance of 119 cm [6]. A case study of an atypical gunshot wound by Verhoff and Karger [7] involved a suicide where extensive backspatter was observed to travel up to 4.6 m. Physical experiments from shots to a bloodied sponge covered in a rigid material resulted in backspatter travelling 30-60 cm [2, 4].

The biological contents of backspatter include brain tissue, bone fragments, skin tissue, adipose tissues and blood. Factors affecting the pattern include muzzle to target distance, calibre of firearm [2] and anatomical location with most studies focused on the cranium.

The significance of backspatter lies in crime scene reconstruction [2]. Specifically, backspatter travels opposite to the line of fire and can therefore be deposited on the firearm, the shooter and surrounding objects. Hence, factors such as weapon type, range of shot [3], blood stain patterns on the hands of victims proving suicides [5], and homicide information may be derived [8].

A key series of experiments by German pathologist Bernd Karger stands out as the most comprehensive study of backspatter [3, 6, 9]. Nine live New Jersey calves (5-6 months old) destined for slaughter were shot in the right temple 10 cm horizontally below the right eye. Key findings included that backspatter results varied with each shot despite a controlled environment but the pattern was a consistent fine mist with every shot immediately after bullet impact. Synthetic models [2, 4] consisting of blood soaked sponges encased in outer coatings produced more reproducible backspatter patterns, were inexpensive and avoided ethical issues. There are several case studies [7, 8, 10, 11] that describe backspatter in non-fatal human shootings, suicides, and homicides. These results can provide a specific situation to validate computational models.

The three main mechanisms that are thought to contribute to backspatter include; (i) subcutaneous gas effects; (ii) temporary cavitation related to intracranial pressure; and (iii) tail splashing. In general, a combination of all three factors may cause backspatter. Subcutaneous gas effects result from pressurized gases during the muzzle discharge [12]. During close range shots the pressurised muzzle gases enter the wound produced by the bullet and become trapped in the subcutaneous space between the skin and skull. This causes ‘starburst or stellate’ entrance wounds in what is known as a ‘blow-out’ effect where the skin mushrooms and a pocket is created under the skin [2, 9]. The hot, pressurised gases expand within this pocket space and create a backwards streaming of gas escaping out of the entrance wound. The accelerating force from the escaping gas drives blood and soft tissue opposite to the direction of fire [2, 4, 9].

Temporary cavitation related intracranial pressure occurs as a bullet passes through a medium creating a temporary cavity in its wake, a feature of all missile wounds [13]. In the case of a bullet wound to the head, a large temporary cavity would be created because of the low retentive forces of brain tissue [13]. The brain is contained within the rigid skull, and therefore as a temporary cavity expands a high pressure is created within the cranium. The high pressure within the cranium and the subsequent collapse of the temporary cavity creates a force to drive tissue and blood back out the entrance wound [7, 9]. Karger proposed that anatomical structures similar to liquid filled cavities provide the best conditions for temporary cavitation [14]. Fackler [15] believed that the collapse of a temporary cavity is the only mechanism that creates backspatter.

The phenomenon of ‘tail-splash’ is the backwards streaming of destroyed material or fluid along the lateral surface of a high velocity bullet as it penetrates a dense medium [9, 13, 14]. Karger [14] suggested that ‘tail-splash’ occurs when a bullet penetrates the brain and lateral streaming of brain matter and blood occurs towards the line of fire. This is most closely related to the mechanism evaluated in this study.

There have been numerous computational studies of high velocity impacts related to ballistics, but little research has been conducted related to backspatter. Finite element analysis (FEA) of ballistic helmet impacts and the effect on the human cranium [16, 17] stresses within the head and brain were used to evaluate the performance of a helmet. FEA studies have simulated particle projectiles in the opposite direction to the line of fire [18-20], which would appear to be backspatter. These are projectile impacts to human bones, namely the parietal bone of the skull [18] and the mandible (jaw) bone [19, 20]. The use of FEA provided good results when compared to experimental data with the relatively simple material models used. Backspatter or its significance was not the focus of those studies. A further FEA study to recreate the wounding that occurred in an actual death [21]

suggested that computer prediction is a useful tool for testing the physics of human ballistic wounding. Many of these studies used LS-DYNA software as the FEA solver [16, 17, 19, 20, 22], and Smooth Particle Hydrodynamics (SPH) [22, 23] was also shown to be useful.

Physical experiments can play crucial roles and are essential to understand the complex mechanisms, characterise the associated material behaviour during backspatter, and validate the computational models. For example, the constitutive relations of biological materials, specifically under high strain rates, are often not known, and need to be determined experimentally. In relation to backspatter, the scope and extent of experiments with animals or animal parts are limited because of ethical and practical reasons. Hence there is an urgent need to develop alternative (simulant) material that will enable conducting large number of experiments to understand backspatter and its relationship to the actual events. The key criterion of simulant material is their properties either individually or in combination need to be close to the biological material (skull, tissue, fluid, etc) relevant to backspatter, and thus they are expected to demonstrate similar events under backspatter conditions. This study focuses on understanding the mechanisms of backspatter and evaluates two simulant materials for human skulls to rate their usefulness as a synthetic material for forensic investigations. Secondly, we evaluate the suitability of a mesh-free method called Smoothed Particle Hydrodynamics (SPH) to model the splashing mechanism during backspatter using a medium density fiberboard (MDF) panel, which is compared to the identical experiment.

## 2. Approach and Methodology

Ballistic experiments were conducted at The Royal New Zealand Police College shooting range in the presence of trained firearms experts. The experimental setup is shown in Fig. 1. In the first experiment a series of  $100 \times 100 \text{ mm}^2$  panels made of Medium density fiberboard (MDF) and Polycarbonate (PC) materials were tested. MDF is made up of wood fibers combined with a resin, and made into panels by applying high pressure and temperature. Polycarbonate was also chosen as the material as it is not brittle and thus would not shatter as a result of projectile impact.



Figure 1. Experimental setup: the physical model was placed on a Kevlar vest with halogen lighting and recorder using a high speed camera.

The assembled physical models were attached to a Kevlar bullet proof vest on a dense foam testing

dummy. The vest and testing dummy was taped to a large flat board to support it and keep the midriff area of the dummy perpendicular to the ground. A table was placed in front of the dummy and the centre of the models taped to the vest 25 cm above the table surface. A 9 mm calibre handgun was used in the experiment with Magtech 9 mm luger centerfire full metal jacket ammunition. The models were shot from a distance of 1 m and fired from a position perpendicular to the model surface. The experiment was filmed with a SA1 high-speed digital video camera with a 55 mm lens and capture rate of 16000 fps. The lighting was achieved with three 1000 W quartz halogen lamps. A large white plastic board was held by clamps behind the model. This board acted as a light reflector to increase the brightness and track the backspatter from the models. Large white sheets of blotch paper were attached for each experiment to the table in front of the models, the plastic board reflector, and the ground immediately around the setup. This was so the spattered particles could be observed and recorded.

### 3. Computational Simulation

Conventional FEA is not suitable for high impact fracture simulations due to a number of factors including capturing the natural crack initiation and propagation, separation of failed elements, maintaining the integrity of elements in highly non-linear deformations, and capturing highly fragmented filamentary crack paths [24]. Consequently, Smooth Particle Hydrodynamics (SPH) was adopted as a suitable method due its mesh free nature. SPH solves a system of partial differential equations with the domain discretised into a series of particles that represent specific material volumes. SPH modelling has been successfully applied to fluid flow problems in the past. More recently there has been a growing interest in modelling solid deformation problems with SPH [24-29]. SPH is ideally suited to modelling the backspatter from a projectile impact due to its proven ability in modelling fractured discrete structures and damage evolution.

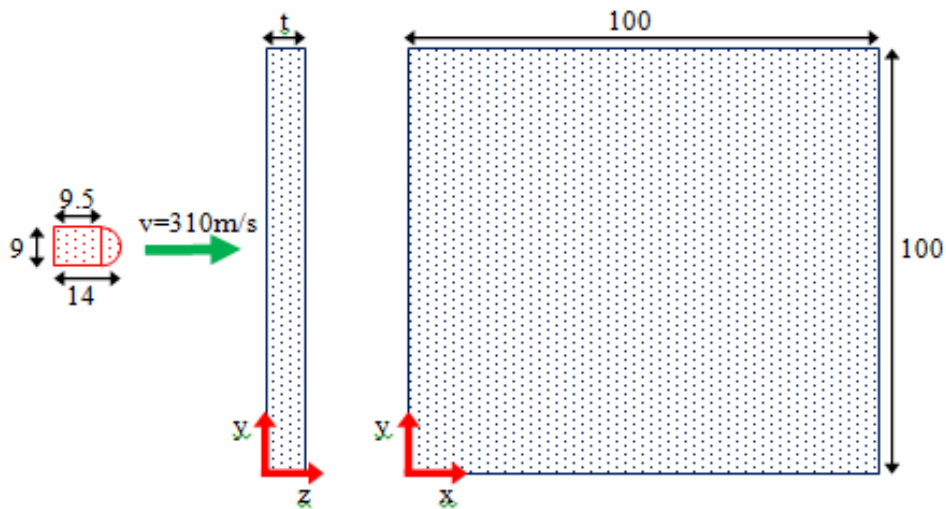


Figure 2. Computational simulation configuration (dimensions in mm, not drawn to scale)

Table 1. Material properties for MDF and polycarbonate used in the computational model

Material	Density	Shear Modulus	Yield Stress	Bulk Modulus	Failure Strain	Reference
MDF	750 kg/m <sup>3</sup>	1357 MPa	42 MPa	2778 MPa	0.5%	[30, 31]
Polycarbonate	1190 kg/m <sup>3</sup>	785 MPa	62 MPa	3010 MPa	100%	[32]

The computational model was setup as shown in Fig. 2. A panel of dimension  $100 \times 100 \text{ mm}^2$  was rigidly fixed at its edges and is impacted by a projectile at its centre. The projectile/bullet shape was simplified as a cylinder, 9 mm in diameter and 9.5 mm long with a semi-hemisphere of radius 4.5 mm at the end. The initial velocity of the bullet was set to 310 m/s. The computational model was simulated for 6 ms after the bullet impact. Both the panel and projectile were discretised with a particle spacing of 1 mm. A particle convergence (equivalent to mesh convergence in FEA) analysis using the von Mises stress showed that the stress varied by less than 2% with a change in model resolution from 1.25 to 1 mm particle spacing, establishing the resolution of 1 mm was sufficiently accurate. Depending on the thickness, the SPH panel was made up of between 61,206 - 71,407 particles and the projectile contained 1,246 particles. The projectile was modelled as solid copper with a Johnson Cook plasticity model [33]. MDF and polycarbonate were modelled using the material properties in Table 1. The model was solved using the LS-DYNA SPH solver.

## 4. Results

### 4.1 High speed impact tests

High speed photographs of a representative example of MDF and PC tested are given in the following section. The behaviour of the simulant materials and the associated advantages and disadvantages in relation to simulating backspatter are summarised in Table 2. For each material, two samples were tested, denoted by MDF1 and MDF2 for the Medium density fiberboard samples, and PC1 and PC2 for the Polycarbonate samples.

Fig. 3 shows the fracture pattern for MDF panels. Small particles (1-2 mm in size) were observed to travel in the direction opposite to the line of fire for both tests. Particles emerged in a radial cone shape with most debris travelling in the upwards direction (Fig. 3c-d). Smaller particles travelled away from the model, whilst larger particles and fragments remained in the region of impact (Fig. 3c). The time for the initial splashing backspatter to occur after bullet impact was 0.28 ms. The backspatter continued to expel from the hole for 6.35 ms. The size of the entrance hole was 9.0 mm with no evidence of radial cracking from the impact site. Large fragments of MDF fractured off leaving damage areas of around 15 mm in diameter at the exit site. Observation of the blotch paper revealed a majority of spattered material was located between 0.5 - 1 m from the model setup.

Two plain 4.5 mm polycarbonate panels as the skull simulant were also tested with PC1 highlighted in Fig. 4. The projectile induced a concave bend in the entire panel. A local radial wave travelled outwards to the edges of the panel 0.19 ms after impact in both cases. Following this the entire panel vibrated sending ripples through the panel. No backspatter was observed for PC panels. The entrance hole was much larger for polycarbonate compared to that observed for MDF.

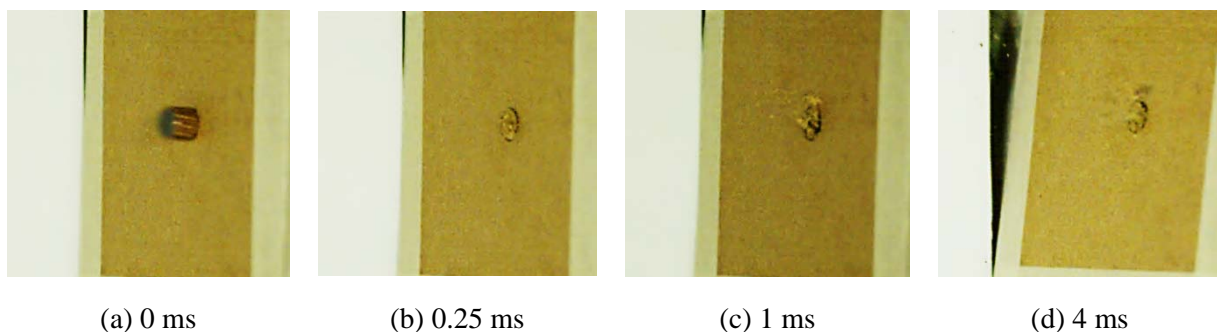


Figure 3. Fracture pattern and backspatter due to projectile impact on MDF (MDF1)

Table 2. Advantages and disadvantages of materials as simulants for human skulls

Material	Advantages	Disadvantages
MDF as a skull/bone simulant	MDF behaves in a brittle manner similar to human bones. MDF produces material backspatter under a high velocity projectile impact. Bone is known to produce similar backspatter [3, 34].	There was no fracture of MDF other than in the area immediately around projectile impact. Fracture lines and cracks are often seen to radiate out from the impact site of a projectile as happens in a skull/bone [35].
Polycarbonate as a skull/bone simulant	There are limited advantages of polycarbonate as a bone simulant.	Polycarbonate did not produce any material backspatter on impact, and there was no material fracture in the form of cracking. The ductile nature of polycarbonate makes it a poor simulant for bone.

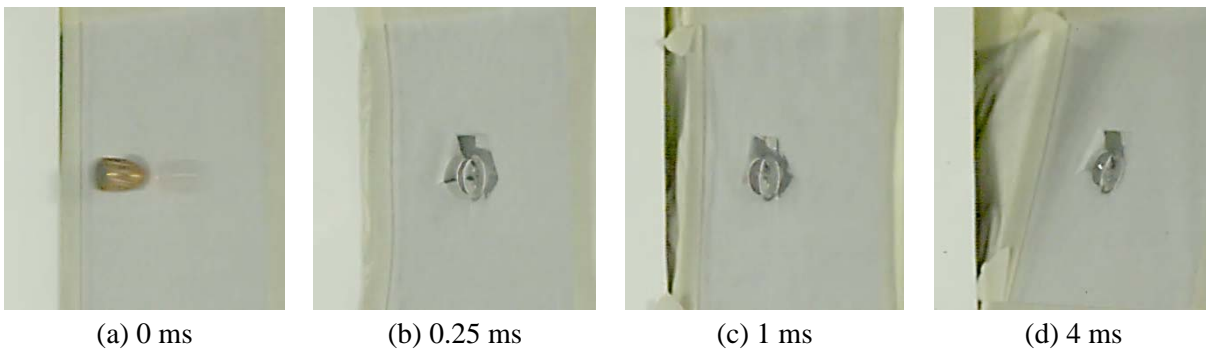


Figure 4. Deformation behaviour during projectile impact on polycarbonate (PC1)

#### 4.2 Computational SPH model of MDF panels

Next we developed a computational model to simulate backspatter using the SPH method. To evaluate the suitability of SPH as an efficient method to capture the impact fracture, fragmentation, post-impact particulate ejection, we simulated the impact of a projectile into a 6 mm MDF panel. Fig. 5 shows the evolution of von Mises stress (left column) and plastic strain (right column) of the plate at various times after the projectile impact. Particle colouring represents a range of 0-20 MPa for von Mises stress and 0-0.5 (failure strain) for plastic strain.

On impact (Fig. 5a) high impact stresses are generated around the projectile tip leading to fracture at the impact point (shown by red particle dispersion). The stressed zone expand radially but are not large enough to produce failure (only 4-12 MPa), and no plastic deformation is noticed outside the fracture site (Fig. 5b). The stress waves reach the plate boundaries, reflect and then dampen. Some fragmented particles at impact have now moved away from the impact site in the opposite direction of the projectile motion leading to backspatter (Fig. 5c-d). The majority of particles clump and fall at the impact site. Failure is only predicted at the impact site.

The SPH model prediction was then compared against the equivalent MDF experiment. Fig. 6 compares the fracture pattern and particle movements against the SPH prediction. Backspatter predictions at 1 and 4 ms show particle movement over a similar distance to the experiment. This means that the velocity of the particles would also be similar. The pattern of spray is also similar representing a 3D cone pattern. The predicted entrance site is also similar to that of the experiment and no fracture is observed away from the impact site in both modelling and experiment.

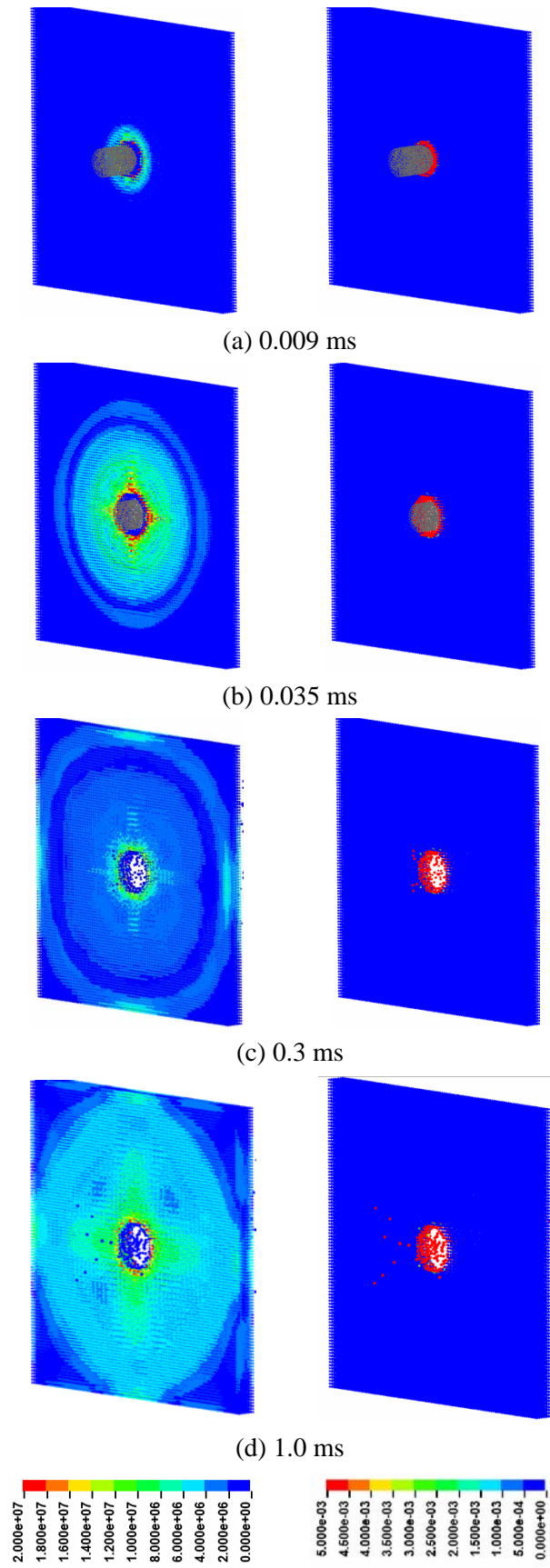


Figure 5. SPH simulation of projectile impact on MDF, left: coloured by von Mises stress (0 - 20 MPa), and right: coloured by plastic strain (0 - 0.006)

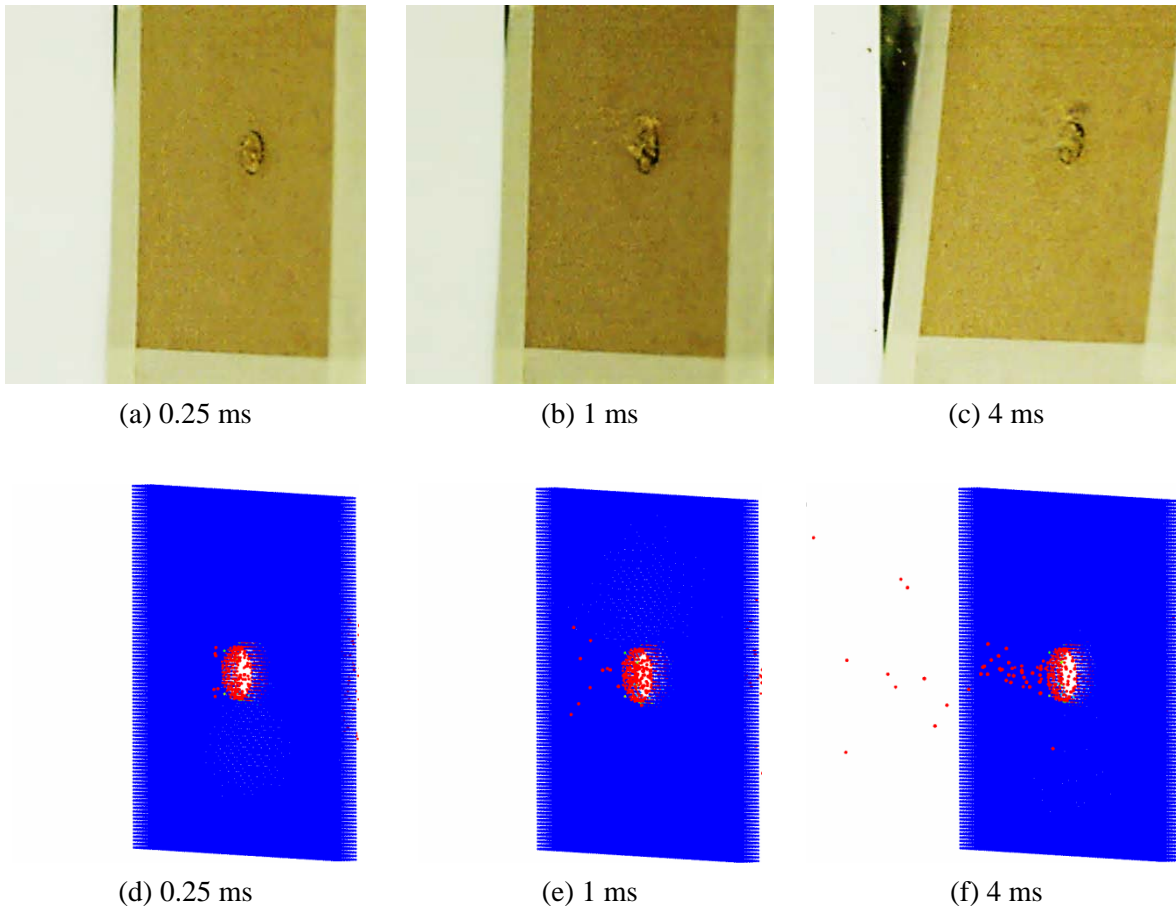


Figure 6. Comparison of experimental (a-c, physical model MDF-1) and computational (d-f) results of projectile impact on MDF (d-f: coloured by plastic strain, red=0.5%)

## 5. Discussion and Conclusions

The study has shown that projectile impact causes fragmentation of material at the impact site, whilst transferring momentum to fragmented particles. The particles travel along the path of least resistance, leading to partial material movement in the opposite direction of the projectile motion, which is known as backspatter. The amount of backspatter depends on the strain limit of each material and the closure time of the initial projectile hole.

SPH was shown to be an ideal numerical method for handling the high impact fragmenting nature of the materials, and the predictions compared well to the experimental data of medium density fiberboard (MDF). Results were also noted to be highly dependent on the constitutive laws. Specifically, the MDF impact fracture results suggest that energy from the projectile causes material at the impact site to fail in a brittle manner with fracture into small particles. Momentum is transferred from the projectile to the particles with the majority of fragments travelling in the original projectile direction. However, for a proportion of the fragments the entrance site acts as the path of least resistance causing material movement axially backwards. This is similar to the tail-splashing mechanism that is postulated as a mechanism of backspatter from a cranial gunshot [9, 13, 14]. The other potential skull simulant, polycarbonate, has a high failure strain and good impact resistance, compared to a real skull, leading to a lack of backspatter and no significant material fracture. Bullet impact in human bones is known to leave a clear hole and shows radial fracture [35] suggesting that polycarbonate is not a suitable simulant for human bone or skull.

This is the first study to use SPH to study backspatter in ballistic impacts. The SPH model

simulated the backspatter particle speed, timing and spray pattern consistent with the same experiment.

Finally from the materials we tested, MDF was found to be best suited to simulating skull/bone. MDF is a better simulant material for skull than polycarbonate under high velocity projectile impact. MDF displays similar brittle properties to bone and produced backspatter. Polycarbonate was very ductile with limited material fracture thus was not a good simulant for bone.

Future work will focus on extending the model to multiple layers and ductile materials. This can be extended to include biological material with an anatomically based human or porcine model. Other mechanisms such as intracranial overpressure and the subcutaneous gas effect have also been theorised. A computational model could be further extended to simulate these mechanisms of backspatter. This would create a more complete model of what happens in reality. This research is thus an important step towards creating a tool to help forensic scientists accurately recreate crime scenes and provide evidence that leads to justice in serious crime investigations.

### References

- [1] R.M. Coupland, M.A. Rothschild, M.J. Thali, B.P. Kneubuehl, R.M. Coupland, M.A. Rothschild, and M.J. Thali, *Introduction to Wound Ballistics*. ed. B.P. Kneubuehl: Springer Berlin Heidelberg 2011, pp. 1-2.
- [2] B.G. Stephens, and T.B. Allen, *Back Spatter of Blood from Gunshot Wounds - Observations and Experimental Simulation*. *Journal of Forensic Sciences*, vol. 28 (2) (1983). pp. 437-439.
- [3] B. Karger, R. Nusse, and T. Bajanowski, *Backspatter on the Firearm and Hand in Experimental Close-Range Gunshots to the Head*. *The American Journal of Forensic Medicine and Pathology*, vol. 23 (3) (2002). pp. 211-213.
- [4] J.O. Pex, and C.H. Vaughan, *Observations of High Velocity Bloodspatter on Adjacent Objects*. *Journal of Forensic Sciences*, vol. 32 (6) (1987). pp. 1587-1594.
- [5] K. Yen, M.J. Thali, B.P. Kneubuehl, O. Peschel, U. Zollinger, and R. Dirnhofer, *Blood-Spatter Patterns: Hands Hold Clues for the Forensic Reconstruction of the Sequence of Events*. *American Journal of Forensic Medicine and Pathology*, vol. 24 (2) (2003). pp. 132-140.
- [6] B. Karger, R. Nusse, H.D. Troger, and B. Brinkmann, *Backspatter from Experimental Close-Range Shots to the Head II- Microbackspatter and the Morphology of Bloodstains*. *International Journal of Legal Medicine*, vol. 110 (1997). pp. 27-30.
- [7] M.A. Verhoff, and B. Karger, *Atypical gunshot entrance wound and extensive backspatter*. *Int J. Legal Med.*, vol. 117 (2003). pp. 229-231.
- [8] M. Kleiber, D. Stiller, and P. Wiegand, *Assessment of shooting distance on the basis of bloodstain analysis and histological examinations*. *Forensic Science International*, vol. 119 (2001). pp. 260-262.
- [9] B. Karger, R. Nusse, G. Schroeder, S. Wustenbecker, and B. Brinkmann, *Backspatter from Experimental Close-Range Shots to the Head I-Macrobackspatter*. *International Journal of Legal Medicine*, vol. 109 (1996). pp. 66-74.
- [10] M.J. Thali, K. Yen, P. Vock, C. Ozdoba, B.P. Kneubuehl, M. Sonnenschein, and R. Dirnhofer, *Image-guided virtual autopsy findings of gunshot victims performed with multi-slice computed tomography and magnetic resonance imaging and subsequent correlation between radiology and autopsy findings*. *Forensic Sci Int*, vol. 138 (1-3) (2003). pp. 8-16.
- [11] S.A. Padosch, R.B. Dettmeyer, C.W. Schyma, P.H. Schmidt, and B. Madea, *Two simultaneous suicidal gunshots to the head with robbed police guns*. *Forensic Science International*, vol. 158 (2-3) (2006). pp. 224-228.
- [12] M.C. Taylor, T.L. Laber, B.P. Epstein, D.S. Zamzow, and D.P. Baldwin, *The effect of firearm muzzle gases on the backspatter of blood*. *International Journal of Legal Medicine*, vol. (2010). pp. 1-12.

- [13] J.J. Amato, L.J. Billy, N.S. Lawson, and N.M. Rich, High Velocity Missile Injury: An Experimental Study of the Retentive Forces of Tissue. *The American Journal of Surgery*, vol. 127 (1974). pp. 454-459.
- [14] B. Karger, Forensic Ballistics. *Forensic Pathology Reviews* 5 2008 pp. 139-172.
- [15] Evaluating Impact Spatter Bloodstains. In *Bloodstain Pattern Analysis with an Introduction to Crime Scene Reconstruction, Third Edition*: CRC Press 2008, pp. 199-229.
- [16] M. Aare, and S. Kleiven, Evaluation of head response to ballistic helmet impacts using finite element method. *International Journal of Impact Engineering*, vol. 34 (2007). pp. 596-608.
- [17] J. Yang, and J. Dai, Simulation-Based Assessment of Rear Effect to Ballistic Helmet Impact. *Computer-Aided Design & Applications*, vol. 7 (1) (2010). pp. 59-73.
- [18] A. Mota, S. Klug, M. Ortiz, and A. Pandolfi, Finite-element simulation of firearm injury to the human cranium. *Computational Mechanics*, vol. 31 (2003). pp. 115-121.
- [19] Z. Tang, W. Tu, G. Zhang, Y. Chen, T. Lei, and Y. Tan, Dynamic simulation and preliminary finite element analysis of gunshot wounds to the human mandible. *Injury, Int J. Care Injured*, vol. 43 (2012). pp. 660-665.
- [20] Z. Tang, Z. Zhou, G. Zhang, Y. Chen, T. Lei, and Y. Tan, Establishment of a three-dimensional finite element model for gunshot wounds to the human mandible. *Journal of Medical Colleges of PLA*, vol. 27 (2012). pp. 87-100.
- [21] J. Raul, C. Deck, F. Meyer, A. Geraut, R. Willinger, and B. Ludes, A finite element model investigation of gunshot injury. *International Journal of Legal Medicine*, vol. 121 (2007). pp. 143-146.
- [22] N. Kilic, and B. Ekici, Ballistic resistance of high hardness armour steels against 7.62mm armor piercing ammunition. *Materials and Design*, vol. 44 (2013). pp. 35-48.
- [23] M. Lee, and Y.H. Yoo, Analysis of ceramic/metal armour systems. *International Journal of Impact Engineering*, vol. 25 (2001). pp. 819-829.
- [24] R. Das, and P.W. Cleary, Effect of Rock Shapes on Brittle Fracture using Smooth Particle Hydrodynamics. *Theoretical and Applied Fracture Mechanics*, vol. 53 (2010). pp. 47-60.
- [25] L.D. Libersky, and A.G. Petschek, Smooth particle hydrodynamics with strength of materials. In *Advances in the Free-Lagrange Method*, ed. Trease and Crowley, Berlin: Springer 1990,
- [26] J.P. Gray, J.J. Monaghan, and R.P. Swift, SPH elastic dynamics. *Computer Methods in Applied Mechanics and Engineering*, vol. 190 (49-50) (2001). pp. 6641-6662.
- [27] R. Das, and P.W. Cleary, Effect of rock shapes on brittle fracture using Smoothed Particle Hydrodynamics. *Theoretical and Applied Fracture Mechanics*, vol. 53 (1) (2010). pp. 47-60.
- [28] R. Das, and P.W. Cleary, A mesh-free approach for fracture modelling of gravity dams under earthquake. *International Journal of Fracture*, vol. 179 (1-2) (2013). pp. 9-33.
- [29] S. Karekal, R. Das, L. Mosse, and P.W. Cleary, Application of a mesh-free continuum method for simulation of rock caving processes. *International Journal of Rock Mechanics and Mining Sciences*, vol. 48 (5) (2011). pp. 703-711.
- [30] A.W.P.A. Incorporated, EWPA Facts about Particleboard and MDF. 2008.
- [31] H. van Dyk 2008. Development of a Wood Fiber Composite using Nonwoven Textile Technology. North Carolina State University.
- [32] J.E. Mark, Polymer Data Handbook. Second. Oxford University Press, 2009.
- [33] G.R. Johnson, and W.H. Cook, Fracture characteristics of three metals subjected to various strains, strain rates, temperatures and pressures. *Engineering Fracture Mechanics*, vol. 21 (1) (1985). pp. 31-48.
- [34] B.R. Burnett, Detection of Bone and Bone-Plus-Bullet Particles in Backspatter from Close-Range Shots to Heads. *Journal of Forensic Science*, vol. 36 (6) (1991). pp. 1745-1752.
- [35] M. Oehmichen, C. Meissner, H.G. Konig, and H.B. Gehl, Gunshot injuries to the head and brain caused by low-velocity handguns and rifles. A review. *Forensic Sci Int*, vol. 146 (2-3) (2004). pp. 111-20.